Int. J. Multiphase Flow Vol. 12, No. 3, pp. 337–355, 1986
Printed in Great Britain

0301-9322/86 $3.00 + .00
Pergamon Journals/Elsevier

EXPERIMENTAL STUDY OF GAS–LIQUID SLUG FLOW IN A SMALL-DIAMETER VERTICAL PIPE

V. E. NAKORYAKOV, O. N. KASHINSKY and B. K. KOZMENKO
Institute of Thermophysics, Siberian Branch of the USSR Acadamy of Sciences,
630090 Novosibirsk, U.S.S.R.

(*Received* 10 *March* 1983; *in revised form* 23 *August* 1985)

Abstract—Experimental investigation of upward gas–liquid slug flow in a vertical pipe in 15 mm ID has been carried out. The electrochemical method which permits the determination of the value and direction of instantaneous wall shear stress as well as the mean and fluctuating components of the liquid velocity is used for measurements. It is shown that the change of the sign of the velocity near the wall usually occurs at the moment of slug passage; the time-averaged wall shear stress at low liquid velocities is significantly lower than the value obtained by means of common prediction methods. The results of measuring of the local void fraction, liquid velocity and components of liquid velocity fluctuations are presented. The time-dependent behavior of the instantaneous hydrodynamic characteristics is described.

1. INTRODUCTION

Gas–liquid slug flow in a pipe is characterized by the existence of gas inclusions whose size is commensurable with the diameter of the pipe. This regime exists within a wide range of flow rate parameters and, typically, has a more complicated structure as compared with the bubble or disperse-annular regimes. Slug flows may be found in many engineering devices (i.e. steam generators, heat exchangers, pipe-lines for combined gas–liquid transport, etc.). Therefore, a great amount of research has been devoted to their study, the most important of which are reviewed in papers by Kutateladze & Styrikovich (1976), Hewitt & Hall-Taylor (1970) and Wallis (1969). The previous research, however, paid attention basically to either averaged characteristics (pressure drop, void fraction) or detailed investigation of gas–liquid characteristics, i.e. sizes and velocities of gas bubbles (Moisis & Griffith 1962; Dukler & Hubbard 1975; Armand 1946). Some local liquid-phase characteristics of the slug flow are studied in papers by Serizawa *et al.* (1975), Inoue & Aoki (1976), Nakoryakov *et al.* (1981). Here the mean velocity and the intensity of liquid-velocity fluctuations were measured along with the local void fraction.

Various structures are meant by the term "slug regime" in the above papers. In the "pure" slug regime the gas phase exists in the flow only in the form of big gas slugs which occupy nearly all the cross-section of the pipe. Liquid plugs between the slugs do not contain gas phase. Such a regime exists in pipes of small diameter at low superficial velocities of the liquid and gas. While increasing the pipe diameter or velocities, a regime appears which has the following structure. The gas slugs lose their regular form and the liquid plugs between them contain a large number of gas bubbles of different size. We will refer to this regime as the "bubble-slug" regime as distinguished from the "pure" slug one. The above papers studied the flow structure mainly in the bubble-slug regime. Our objective was to make similar measurements in the "pure" slug regime.

This paper presents results of an experimental study on the basic turbulent characteristics of a slug flow in a 15-mm-diam. vertical pipe within the range of superficial liquid velocities from 0.12 to 1.2 m/s. Profiles of local void fraction and liquid velocity as well as the intensity of liquid velocity fluctuations were measured in the experiments. Special attention was paid to the investigation of the instantaneous wall shear stress distribution. The measurements were performed by an electrochemical method (Hanratty 1967; Kutateladze *et al.* 1968).

2. EXPERIMENTAL PROCEDURE

2.1 Experimental set-up

The measurements were made on an installation whose diagram is given in figure 1. It is a closed liquid flow loop. The test section is a vertical 15-mm-diam. 4.5-m long pipe

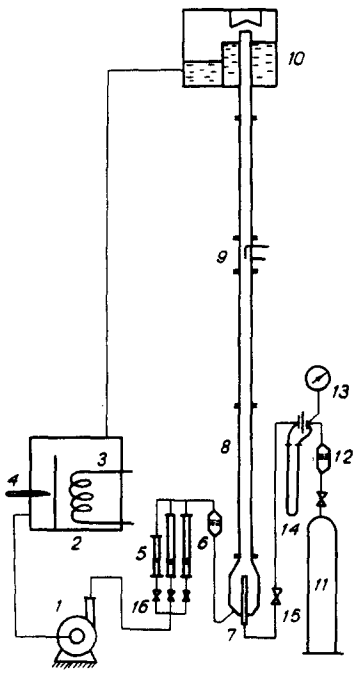

Figure 1. Schematic diagram of experimental set-up. 1, pump; 2, storage tank; 3, heat exchanger; 4, termometer; 5, rotameter; 6, filter; 7, gas supply; 8, test section; 9, measuring section; 10, separator; 11, pressure vessel; 12, air filter; 13, manometer; 14, orifice meter; 15,16 controlling valves.

made of plexiglass. The maximum liquid velocity is 2 m/s. The liquid flow rate was measured by a system of rotameters allowing to cover the superficial velocity range of 0.03–2 m/s. The temperature of the liquid was maintained constant by an automatic controller at the level of 20 $\pm$ 0.2°C. The gas was supplied to the flow through a 8-mm-diam. nozzle installed at the inlet of the test section. Nitrogen was fed from high-pressure cylinders. The flow rate was measured with the help of an orifice meter and a U-type differential manometer.

The flow characteristics were measured at the distance of 2.5 m from the beginning of the test section. The measurement unit contained a wall shear stress probe and a velocity probe located over one cross-section on the pipe. The velocity probe was shifted by a traversing mechanism, the coordinate being measured by an indicating gauge with the accuracy of 0.01 mm.

The test liquid was a standard electrochemical solution of 0.5-N sodium hydroxyde and 0.01-N potassium ferricyanide and ferrocyanide in distilled water.

2.2 Measurement technique

The use of the electrochemical method to study gas–liquid flows was described in detail by Nakoryakov *et al.* (1981). To measure the local void fraction and liquid velocity, the authors used a "blunt-nose" probe with the external diameter of 0.04 mm and the diameter of the platinum electrode of 0.02 mm. The procedure of measuring the liquid velocity is completely analogous to that described in the above paper.

The slug flow can be characterized by a high intensity of fluctuations near the wall. In particular, at some moments of time the velocity near the wall may change its sign. Therefore, a special procedure to measure the wall shear stress was used, which is analogous to that applied by Karabelas & Hanratty (1968) that makes it possible to measure not only the value, but also the sign of the wall shear stress.

A double-wall shear stress probe was used which consisted of two platinum electrodes of size 0.02 $\times$ 0.3 mm^2 welded into the glass at the distance of 0.015 mm one from another (figure 2) and polished flush with the pipe wall. During the simultaneous operation of both electrodes in the presence of a liquid flow, the diffusion wake of the first electrode "shields" the electrode located downstream, so the readings of the latter turn out to be

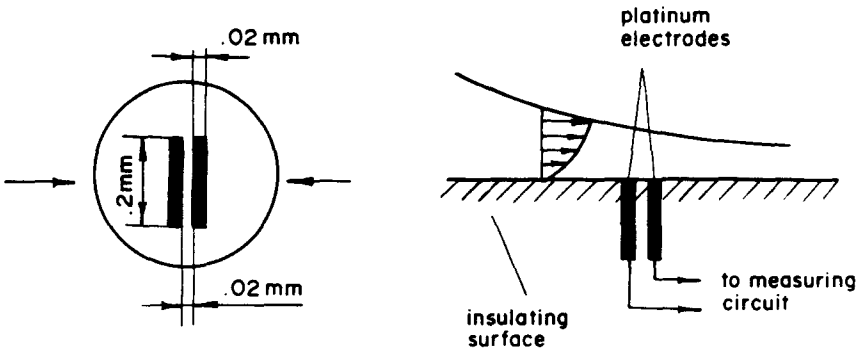

Figure 2. Double electrochemical wall shear stress probe. 1, platinum electrodes; 2, insulating surface; 3, to measuring circuit.

lower. When the flow changes its direction, the smaller current value corresponds to the first electrode. Since the electrodes of the probe are of small size and closely spaced, their hydrodynamic conditions are identical, and they must read the same current values while operating independently.

To preliminarily process the signals of the double probe an electronic circuit was used which is given in figure 3. The current of electrodes 1,2 of the double probe was amplified by dc amplifiers 3,4 with adjustable gains necessary for the initial balancing of the probe currents due to some inevitable difference in their geometrical dimensions. The output voltage of amplifiers 3,4 was fed to differential amplifier–comparator 5. The output voltage of the comparator was +5 V, if the output voltage of amplifier 3 was greater, i.e. in case when the second electrode was in the wake of the first one. While changing the direction of the flow, the first electrode was in the wake of the second one and the output voltage of the comparator was −5 V. This voltage controlled electronic switch 6 which applied to output amplifier 9 the signal of the channel whose electrode happened to be first at a certain moment of time, the voltage of the first channel having been preliminarily inverted by inverter 7. Frequency meter 8 allowed us to determine the time fraction when a reverse flow exists in the probe.

The output signal of the above circuit has the form given in figure 4. The portions of the signal above the zero line correspond to the alternating wall shear stress in the case of the forward direction (the liquid near the wall moves upwards). The negative values of the signal correspond to the reverse flow (the liquid near the wall moves downwards). Considerable jumps of the signal during the change of sign (instead of a smooth transition through zero) are due to the existence of a nonlinear dependence between the probe current and the wall shear stress.

Figure 5 shows a calibration curve for the wall shear stress probe (the output voltages of the amplifiers of both channels vs wall shear stress). Since both channels have been previously balanced, the calibration curves of the first and second probes are the same if they operate independently. With simultaneous turning on of the probes, the readings of the downstream one fall by about 15% for all liquid velocities.

The schematic diagram of the measurement equipment is given in figure 6. The amplified signals of the velocity probe and the voltage of the output amplifier of the circuit 3 were

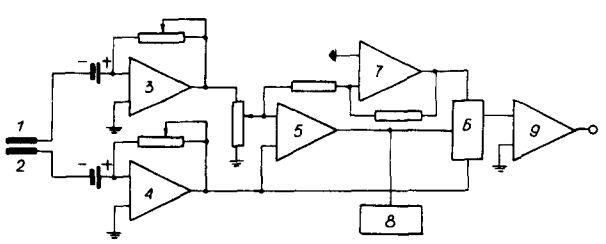

Figure 3. Electronic circuit for processing of the double probe signal. 1,2, electrodes of the probe; 3,4, dc amplifiers; 5, differential amplifier; 6, electronic switch; 7, inverter; 8, frequency meter; 9, output amplifier.

Figure 4. Signal of alternating-sign wall shear stress probe. Vertical axis, voltage; horizontal axis, time (arbitrary units).

recorded on Schlumberger MP 021 magnetic tape recorder 5. While reproducing the signals recorded they were amplified and fed to a two-channel AD transformer of a computer M-6000. Subsequently the signals were processed in the digital form.

The friction and velocity probes were calibrated in the case of single-phase flow in the pipe. In so doing, the velocity probe was installed on the axis. The mean liquid velocity was varied during the calibration within the ranges of 0.03–0.12 and 0.3–2 m/s, i.e. the range of the transition flow in the pipe was excluded. The wall shear stress was determined on the basis of the Haagen–Poiseuille relation and from the Blasius relation according to the liquid flow rate. Single calibration curves were plotted for all the velocity range. Immediately after the experiment a recalibration was carried out. Typically, the difference between the first and the second calibrations did not exceed 1% in probe current; otherwise the measurements were repeated.

To illustrate the accuracy of the procedure described, figure 7 shows a velocity profile measured for a laminar flow in the pipe for the Reynolds number of 1000. The maximum deviation of the experimental points from the theoretical parabolic profile did not exceed 1%.

To control the accuracy of liquid-velocity measurements in a two-phase flow, the measured local velocity integrated over the cross-section was compared with the velocity determined from the flow rate. For the regimes in which the velocity measurements had been carried out the difference did not exceed 7% (partly it can be accounted for by the presence of backward flows near the wall whose consideration lay beyond the limits of the liquid-velocity measurement procedure applied).

3. MEASUREMENT RESULTS

3.1 General flow structure. Parameters measured

The two-phase flow parameters were determined for the superficial liquid velocities $\mathscr{V}_l$ = 0.12, 0.3, 0.4, 0.6 and 1.2 m/s. The gas flow rate was varied for each liquid velocity from a minimum value at which a slug flow appeared (big bubbles in the form of a "spherical

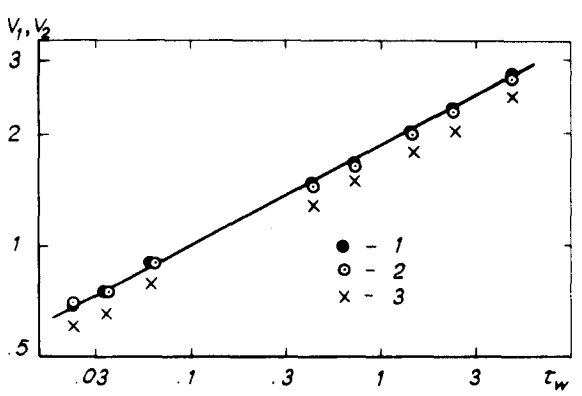

Figure 5. Calibration of double-wall shear stress probe. 1,2, electrodes 1,2 when operating independently; 3, downstream electrode at joint operation V_1, V_2, volts; τ_w N/m².

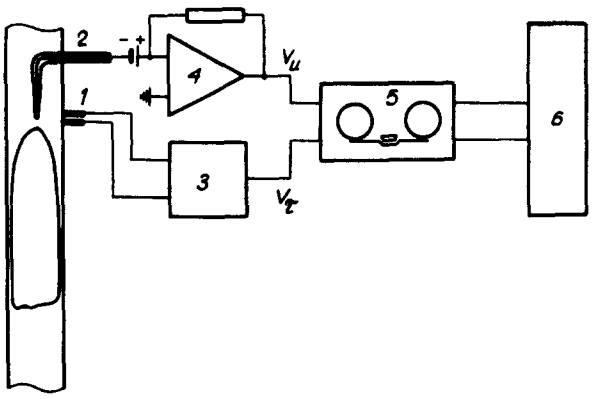

Figure 6. Circuit of the measuring system. 1, wall shear stress probe; 2, velocity probe; 3, electronic circuit (figure 3); 4, dc amplifier; 5, tape recorder; 6, electronic computer.

cap" occupied nearly all the cross-section of the channel) and up to a maximum value which corresponded to the values of the mean void fraction $\alpha_m = 0.5/0.6$. The wall shear stress and the local void fraction profiles were measured in all the regimes. The velocity profiles were measured only at $\mathscr{V}_l \geqslant 0.4$ m/s.

Figure 8 shows a typical fragment of the simultaneous record of the output voltages V_τ and V_u (figure 6) proportional to the diffusion currents of the wall shear stress and of the velocity probes, respectively, the latter having been placed on the pipe axis. The vertical-axis scales are arbitrary, and direction of the time axis is from left to right. The oscillogram shows that during the moments when a gas slug passes through the given cross-section (sharp drop of V_u), the local wall shear stress rapidly decreases. At a certain distance from the beginning of the slug the sign of V_τ changes, which corresponds to the existence of a downward flow near the wall. Then the acceleration of the backward flow occurs, and it is only some time after the passage of a gas slug that the flow changes its sign again (forward direction). The schematic diagram of the flow is presented in figure 9. The slug lifts above the pipe wall at a certain velocity $\mathscr{V}_B$. If one passes to a frame of reference associated with the moving slug, then as a first approximation, we have the free fall of the liquid, with the initial velocity $\mathscr{V}_0$ equal to the velocity with which the bubble moves with respect to the liquid. At a point A the free-fall speed attains $\mathscr{V}_B$, so in the laboratory coordinate system this point is characterized by the zero velocity. Then the falling film is

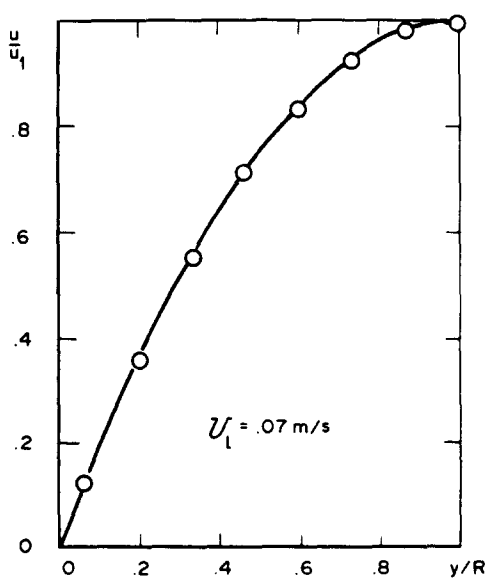

Figure 7. Velocity profile in a single-phase flow. Solid line, parabolic distribution.

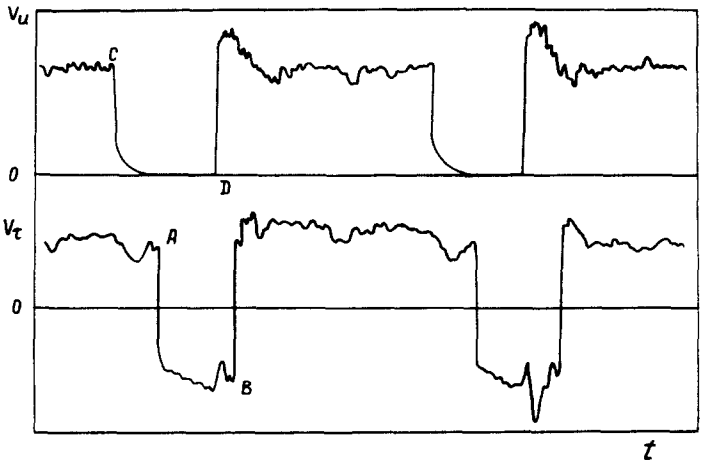

Figure 8. Fragment of synchronous record of signals of wall shear stress and velocity probes. V_u, V_τ, volts; t, s.

accelerated and, possibly, stabilized under the action of the friction force at the wall (if the slug is long enough).

When a liquid plug begins to pass through the given cross-section D, at the first moment of time the liquid near the wall in the thin layer moves downwards, whereas in the center of the pipe the liquid, naturally, moves upwards. In some period of time the downward jet is "smeared" by the upward flow (point B), and the flow over the entire cross-section becomes upward again until the next slug arrives.

The simultaneous records of the wall shear stress and velocity probe signals show that in increasing the liquid velocity, the portions of the backward flow become shorter and the sign does not change with every slug. It is quite natural, since in this case the gas-slug velocity increases, and to accelerate the liquid in the film up to $\mathscr{V}_B$, it is necessary that

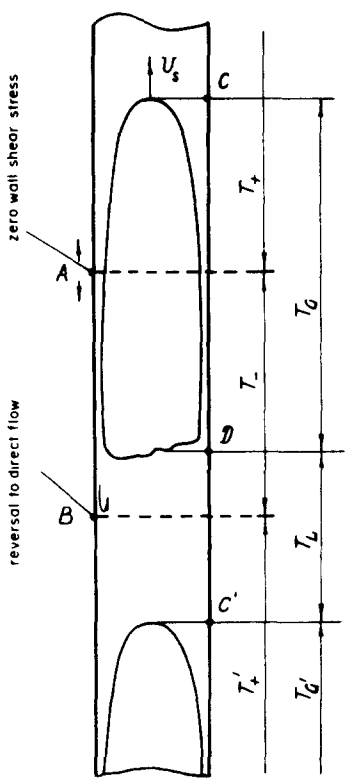

Figure 9. Scheme of slug flow. Points A,B,C,D correspond to those of figure 8.

the slug length should be great. When the liquid velocity was 1.2 m/s, only the longest slugs caused transitory back flows near the wall.

As a result of the digital processing of the signals from the friction and velocity probes using the calibration curves measured, the following flow characteristics were determined: The void fraction on the axis (α_a), the back flow coefficient (f_B), the intensities of the forward and of backward wall shear stress (τ_+, τ_-), the mean value of the wall shear stress (τ_w),

$$\begin{aligned}
\alpha_a &= T_G/T \quad , \\
f_B &= T_-/T \quad , \\
\tau_+ &= \frac{1}{T(1-f_B)} \int_{T_+} \tau(t)\, dt \quad , \\
\tau_- &= \frac{1}{T f_B} \int_{T_-} \tau(t)\, dt \quad , \\
\tau_w &= \frac{1}{T} \int_{T} \tau(t)\, dt \quad , \\
\tau_L &= \frac{1}{T} \int_{T_L} \tau(t)\, dt \quad , \\
\tau_G &= \frac{1}{T_G} \int_{T_G} \tau(t)\, dt \quad .
\end{aligned} \tag{1}$$

Here T is the total time of the measurement, T_+, T_- are the times of the existence, over the given cross-section, of forward and backward flows near the wall, T_L, T_G are the times of the presence, over the given cross-section, of the liquid and of the gas phase. The values T_+, T_-, T_L, T_G for one ith slug are given in figure 9. $\tau(t)$ is the instantaneous value of the friction stress at a moment of time t.

In measuring the local void fraction and velocity profiles $\alpha(y)$ and $u(y)$, the calculations were performed according to the analogous formulae

$$\begin{aligned}
\alpha &= T'_G/T \quad , \\
u &= \frac{1}{T(1-\alpha)} \int_{T_L} u\, dt \quad ,
\end{aligned} \tag{2}$$

where T'_L and T'_G are the times of existence of the liquid and gas phase at a given point.

The following evident relation is valid:

$$\tau_w = (1 - f_B)\, \tau_+ + f_B \tau_- \quad , \tag{3}$$

where $\tau_- < 0$. The mean void fraction α_m was determined by integrating the local void fraction over the cross-section of the pipe. α_m corresponds to the "actual void fraction" measured, e.g. by the cutoff method.

The dependence of α_m on the parameter $\mathscr{V}_g/(\mathscr{V}_l + \mathscr{V}_g)$ obtained in our experiments is given in figure 10. Armand (1946) suggested the well-known relation $\alpha_m = 0.833 \times \mathscr{V}_g/(\mathscr{V}_l + \mathscr{V}_g)$ for horizontal pipes. Mamayev *et al.* (1978) showed that for large values of Froude number the relation $\alpha_m = 0.81\ \mathscr{V}_g/(\mathscr{V}_l + \mathscr{V}_g)$ is valid for vertical pipes. The results of our experiments yield for $\mathscr{V}_l > 0.6$ m/s a deviation from Mamayev's dependence by about 5%. It seems to be due to an error in determining the actual void fraction by integrating the local gas content over the pipe cross-section. It is natural that subsequently at low superficial liquid velocities $\mathscr{V}_l < 0.6$ m/s the experimental points deviate downwards, which is due to the departure from the self-similarity regime (Mamayev *et al.* 1978).

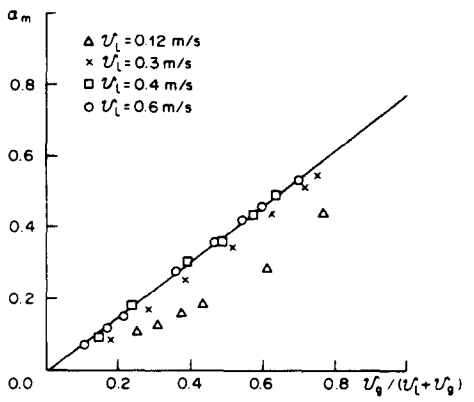

Figure 10. Mean cross-sectional void fraction.

3.2 Wall shear stress characteristics

Figure 11 shows the dependence of the backward-flow coefficient on the mean void fraction. The value f_B increases with increasing the void fraction and strongly depends on the liquid velocity $\mathscr{V}_l$. At $\mathscr{V}_l = 0.6$ m/s, $f_B = 0$ up to the certain value α_m. The length of gas slugs in these regimes is not sufficiently great, and the liquid velocity has no chance to change its sign.

It should be noted that for liquid velocities $\mathscr{V}_l > 0.4$ m/s the relation $f_B < \alpha_m$ is valid, i.e. the backward flow occurs only during a certain time fraction when a slug passes through the given cross-section. At $\mathscr{V}_l = 0.12$ m/s, f_B is considerably greater than α_m. In this regime even at minimum α_m after the passage of small slugs-bubbles there appear powerful backward flows of considerable duration. The coincidence of f_B and α_m at $\mathscr{V}_l = 0.3$ m/s is, of course, accidental.

Figure 12 shows intensities of the forward and of the backward flows for different liquid velocities. The values τ_+ and τ_- are of purely methodical interest. They show what contribution the existence of the backward flow makes to the mean wall friction stress measured. It is interesting to note that for great α_m, τ_- are described, as a first approximation, by close dependences irrespective of the liquid velocity (at $\mathscr{V}_l > 0.3$ m/s). τ_- is the time-average value from the instantaneous values of τ_w, beginning with the point at which the instantaneous value of $\tau_w = 0$, and up to a negative τ_w, maximum for a given gas slug.

Assuming that the relative slug velocity $\mathscr{V}_0 = 0.48\,(gR)^{1/2}$, we will get in accordance with Batchelor (1970), a limiting value of τ_w corresponding to the stabilized fall of a liquid film equal to 5.4 N/m^2.

Figure 12 shows that for $\mathscr{V}_l = 0.3$ m/s and maximum α_m, τ_- approaches the limiting value.

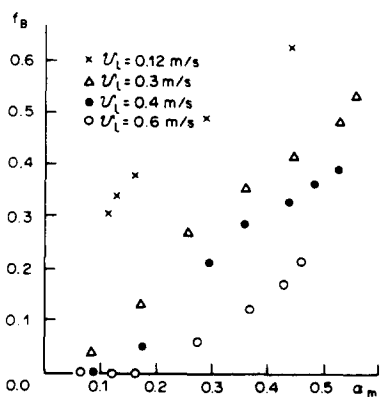

Figure 11. Backward flow index.

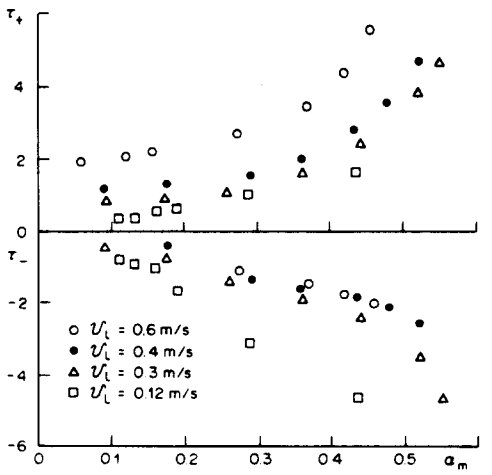

Figure 12. Intensities of forward and backward wall shear stress. τ_+, τ_-, N/m^2.

The wall shear stress averaged during the entire experiment, τ_w, is shown in figure 13 in the coordinates τ_w/τ_0 (where τ_0 is the wall shear stress in the case a single-phase flow with the mean velocity equal to $\mathscr{V}_l$) vs α_m. Here Armand's (1946) relation is also given:

$$\tau_w/\tau_0 = (1 - \alpha_m)^{-1.53} \quad . \qquad [4]$$

The figure shows that the results of our experiments are in good agreement with Armand's formula at $\mathscr{V}_l > 0.6$ m/s. At lower liquid velocities, experimental points considerably deviate downwards from the above dependence. It should be noted that the behavior of $\tau_w(\alpha_m)$ at $\mathscr{V}_l > 0.4$ m/s is qualitatively analogous to that given in a paper by Cognet *et al.* (1978). At lower liquid velocities τ_w drops with increasing α_m and has a qualitatively different pattern as compared with Armand's relation. The mean wall shear stress at $\mathscr{V}_l = 0.12$ m/s is negative in all the regimes, and its absolute value is greater as compared with τ_0.

Let us also note the peculiarity of the behavior of $\tau_w(\alpha_m)$ at $\alpha_m < 0.2$. At small void fractions τ_w grows more rapidly than [4] predicts. τ_w/τ_0 attains the value 1.4–1.6 at $\alpha_m = 0.1$ and then becomes approximately constant or slightly drops before the meeting with [4]. Such a behavior at small void fractions was pointed out by Nakoryakov *et al.* (1981) and Aoki & Inoue (1976) for the case of the bubble flow regime. It should be noted that at $\alpha_m < 0.2$ we have a regime which can be classified as the bubble regime (bubbles in the form of a "spherical cap" have the size close to the diameter of the channel).

If the wall shear stress had been measured by a conventional electrochemical method using a single probe, we would have obtained appreciably overestimated values for the mean wall shear stress. At the cost of "rectifying" the measurement results would have been

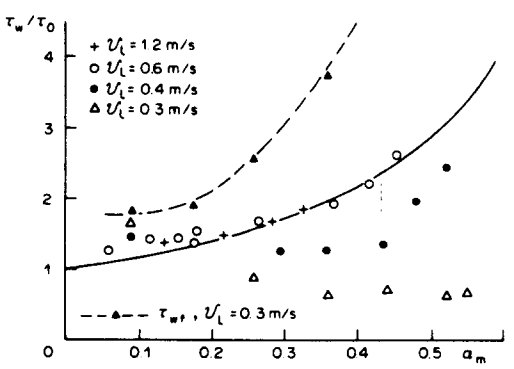

Figure 13. Mean wall shear stress. Solid line, dependency [4].

described by [3], with the opposite sign of the second term in the right-hand side. This ficticious value of the mean wall shear stress τ_{wf} is also given in figure 13. Such a methodical measurement error may be one of the reasons for a considerable increase in wall shear stress at the velocities of 0.22 and 0.44 m/s as compared with [4] described by Nakoryakov *et al.* (1981).

Figures 12 and 13 show that at low liquid velocities the mean wall shear stress τ_w is an algebraic sum of two addends whose absolute values are large. At $\mathscr{V}_l = 0.3$ m/s (and the more so at $\mathscr{V}_l = 0.12$ m/s) the absolute values of τ_+ and τ_- are much greater than τ_0 for these liquid velocities. For that reason the resulting values of τ_w are sufficiently unstable, even small changes of τ_+, τ_- and α_m result in considerable changes in τ_w. So in the range $|\tau_w|/\tau_0 < 1$, the results are sufficiently unstable. In case when either positive or negative contributions to τ_w dominate, experimental results become well reproducible again.

3.3 Local void-fraction and liquid-velocity profiles

In the experiments by Serizawa *et al.* (1975) and Nakoryakov *et al.* (1981) performed on pipes of large diameter, the radial void fraction distributions in the slug regime were close to the parabolic one. However, these works studied the mixed "bubble-slug" regime in which it was difficult to distinctly single out gas slugs and bubbles contained in liquid plugs. In our experiments gas slugs had a well-defined shape which is schematically shown in figure 9.

Our results given in Figure 14 show a quite another form of the dependence $\alpha(r)$. At large α_m in the pipe center α is practically constant and decreases rapidly near the wall.

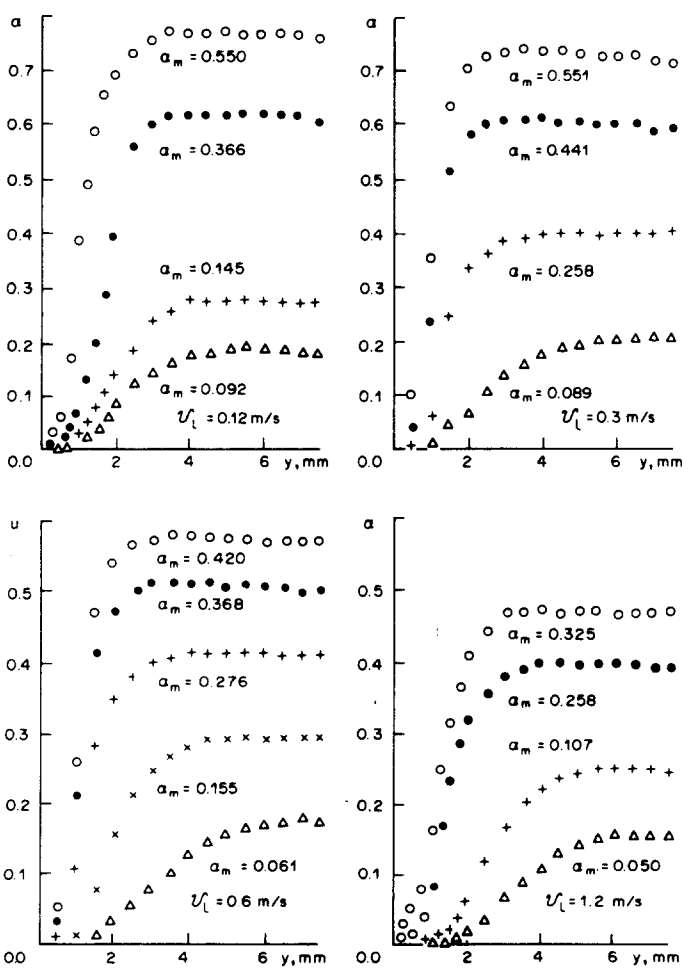

Figure 14. Local void fraction.

To some extent $\alpha(r)$ are close to the parabolic distributions for the lowest void fractions $\alpha_m = 0.1-0.2$ with bubbles in the form of a "spherical cap." However, in this case there exists a sufficiently large near-wall region with $\alpha = 0$ whose width increases with increasing $\mathscr{V}_l$ up to nearly 2 mm. It occurs at the cost of driving the bubbles from the wall when increasing the fluctuating liquid velocity. In the bubble regime this effect results in a transition from the saddle-like radial distribution of void fraction to the parabolic one.

The peculiarity of the distributions of $\alpha(y)$ at large α_m is weakly defined, but still a noticeable trend to a slight decrease of α to the pipe center as compared with the intermediate radii. At large α_m liquid plugs, typically, contain many gas bubbles, and the above trend may be a result of an increased concentration of bubbles near the pipe wall.

Liquid velocity profiles measured for different velocities $\mathscr{V}_l$ are given in figure 15. Figure 16 shows the same profiles in the dimensionless coordinates. In all the regimes the velocity profiles are less filled as compared with the single-phase profile. As $\mathscr{V}_l$ increases, the velocity profiles approach the single-phase profiles. The behavior of the velocity profiles in our experiments is absolutely the same as in the experiments performed on tubes of large diameter.

The above velocity profiles were measured in the regimes where the backward flow coefficient either was equal to zero or did not exceed 0.2. In those regimes where f_B was not equal to zero the measured points which were closest to the wall might be over-estimated. The actual profile near the wall would be even less filled.

Figure 17 shows the values of the local liquid flow rate $u(1-\alpha)$ characterizing the distribution of the flow rate over the pipe cross-section. At $\mathscr{V}_l = 0.4$ and 0.6 m/s near the wall, $u(1-\alpha)$ have the same distribution for different α_m and the same $\mathscr{V}_l$. In the central

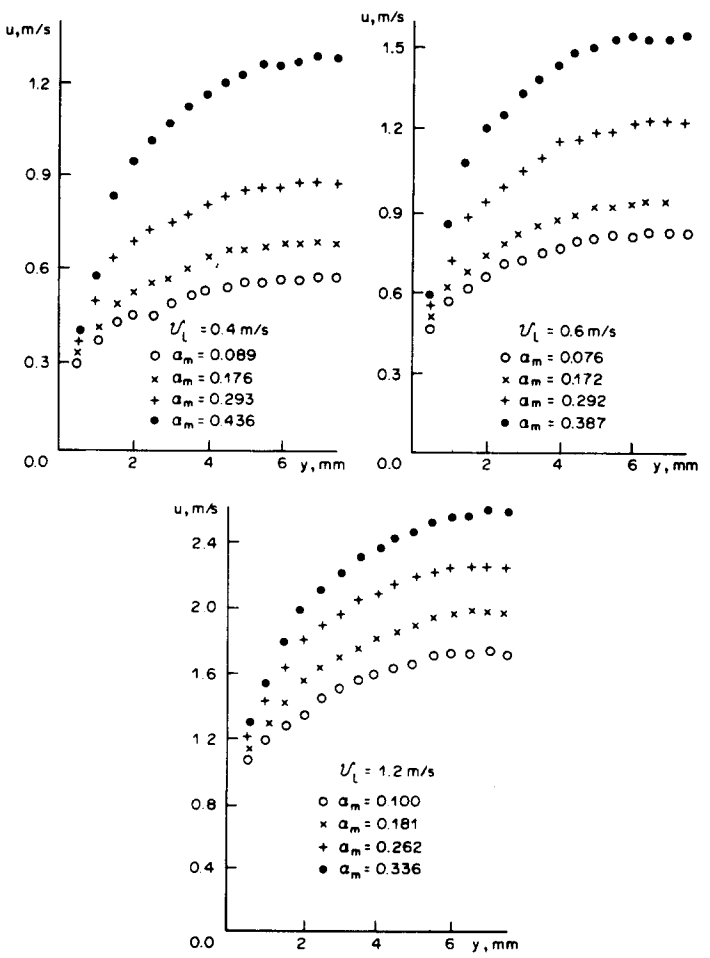

Figure 15. Local velocity of liquid. u, m/s; y, mm.

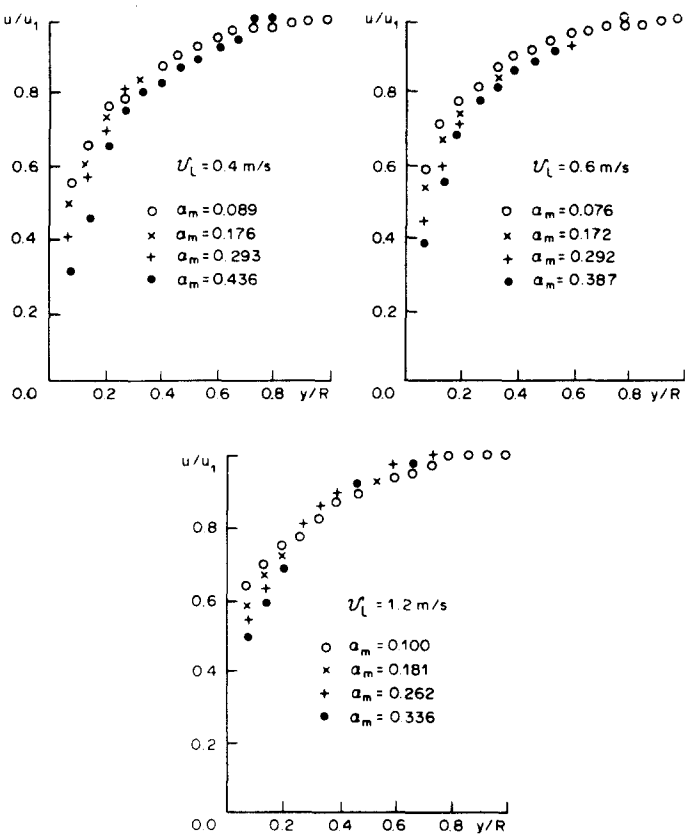

Figure 16. Reduced liquid-velocity profiles.

part of the pipe a separation of the points can be observed for different void fractions. At small α_m the local velocity is practically constant along the entire radius of the pipe, excluding the near-wall region. At $\mathcal{V}_l = 1.2$ m/s the behavior of $u(1-\alpha)$ is more complicated, and the local flow rate ceases to monotonously depend on y, and there is a separation with respect to α_m.

3.4 Fluctuating flow characteristics

As is known (Hanratty 1967), the wall shear stress in a single-phase turbulent pipe flow fluctuates around a mean value, the relative intensity of the fluctuations being about 0.3. In a two-phase flow the intensity of friction fluctuations essentially grows. Strictly

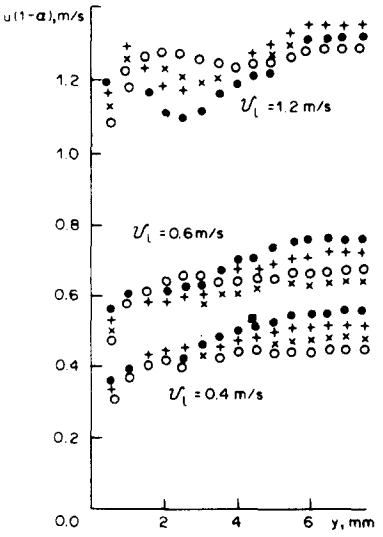

Figure 17. Local liquid flow rate. u, m/s; y, mm.

speaking, the value $\tau' = \sqrt{[\tau(t) - \tau_w]^2}$ is not now a fluctuating component superimposed on the mean value, since τ'/τ_w can be considerably greater than unity and attain very high values for the regimes when $\tau_w \simeq 0$. τ' is the simplest characteristic determining the scatter of the instantaneous values of $\tau(t)$ around the mean value. The measured values of this parameter are given in figure 18. As distinguished from the mean value, τ' increases monotonously in all the regimes and for different values of liquid velocity and the same α_m, the values of τ' do not differ very much one from another, since the mean values of τ_w at different $\mathscr{V}_l$ may differ several times. One should note the nonmonotonous pattern of the curve τ' depending on α_m vs $\mathscr{V}_l$.

Figure 19 shows values of turbulence index $\epsilon_u = u'/u$ of liquid velocity in a slug flow. The intensity of the fluctuations has been related to the mean local liquid velocity at a given point. The behavior of ϵ_u is qualitatively similar to the behavior of this parameter in a bubble flow. In the central part of the pipe where $r/R < 0.75\epsilon_u$ is practically constant along the radius. Near the wall ϵ_u sharply increases. The values of the turbulence index increase with increasing the void fraction. Unlike the bubble flow (Serizawa *et al.* 1975), ϵ_u turns out to be constant in the central part of the pipe, since the mean velocity value falls noticeably (figure 15).

The absolute values of u' behave in a more complicated manner (figure 20). u' attains its minimum for an intermediate value of the radius and increases if moving from the pipe axis to the wall. As void fraction increases, this trend makes itself felt more appreciably. Therefore, the fact that ϵ_u is constant in the central part of the pipe seems to be accidental, since both the absolute intensity of the fluctuations, and the mean velocity vary in this range approximately in the same manner.

Figure 20 also shows the first results for the intensity of the transverse liquid-velocity fluctuation component measured in a two-phase slug flow. v' was measured by a V-shape double electrochemical velocity probe (Nakoryakov *et al.* 1980). Here the measurement procedure is similar to that described by Kashinsky *et al.* (1981). Test measurements in a single-phase flow are also described there.

As distingished from the longitudinal fluctuation component which considerably increases as compared with the single-phase values, the effect of the gas phase on the transverse velocity fluctuation is rather weak. The values of v'/u_1 fluctuates within the range of 0.34–0.48 and are nearly constant over the cross-section of the pipe, excluding the near-wall region. In the case of a single-phase pipe flow v'/u_1 is known to range within 0.34–0.4 (Laufer 1954).

Such a behavior of the intensities of velocity fluctuations components in a slug flow is analogous to the results of measurements in a quasiturbulent bubble flow at low Reynolds numbers (Kashinsky *et al.* 1981). In both cases the disturbing effect of the gas phase due to the relative motion of gas bubbles or slugs in the liquid excites only the additional longitudinal velocity component, weakly affecting the transverse one. These results confirm the hypothesis (Elin & Klapchuk 1980; Sato & Sekoguchi 1975) that a two-phase flow (especially in the slug regime) is an unsteady-state turbulent flow, its unsteady-state characteristics (or the large-scale component of the process) are not correlated with the intrinsic turbulence of the liquid.

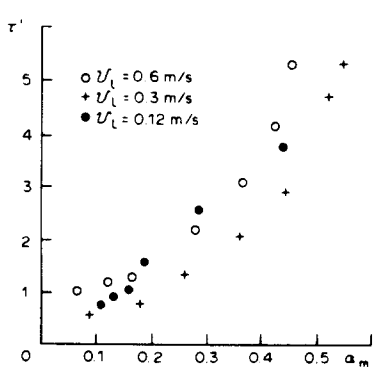

Figure 18. Wall shear stress fluctuations intensity. τ', N/m^2.

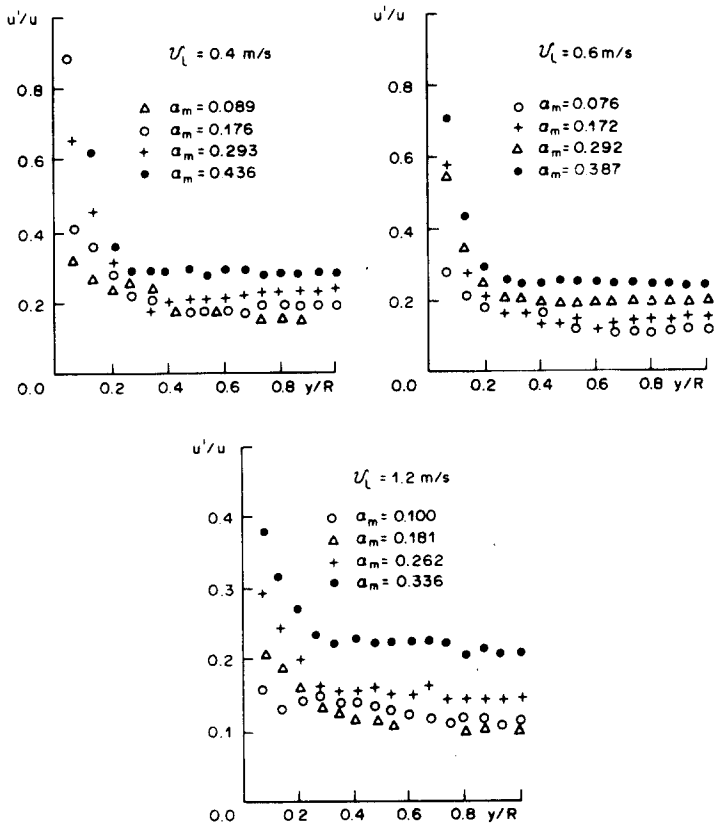

Figure 19. Turbulence index of liquid velocity in a two-phase flow.

3.5 Flow in liquid plugs

Since the slug-flow characteristics differ substantially depending on either liquid plug or gas slug passes at a given cross-section, it seems to be interesting to study these cases separately. Some conditional characteristics of liquid-plug flow will be given in this section.

Another velocity probe was installed on the pipe axis. This probe was intended to determine the moment of the passage of a liquid plug. In a gas phase the signal of the

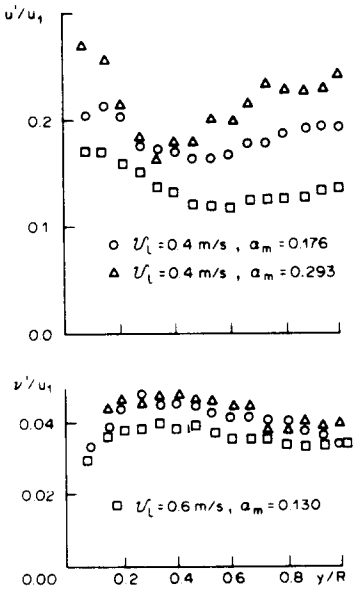

Figure 20. Longitudinal and transverse fluctuations of liquid velocity.

probe decreases up to zero. When analyzing the signal of the probe located on the pipe axis, it was necessary to distinguish between a slug and the gas bubbles contained in the liquid plug. In was performed on the basis of the duration of a signal due to the gas phase. This gas inclusion was considered as a slug, if its duration exceeded a predetermined value corresponding to the size of a gas bubble equal to the pipe diameter. Fortunately, the selection of the criterion to distinguish a gas slug was not critical to the predetermined value of the time interval, since the sizes of the gas slugs and bubbles contained in liquid plugs differ at least 5–10-fold. Let us point out once more that gas slugs and plugs were identified by the probe installed on the pipe axis.

The local void-fraction profiles in a liquid plug φ_p given in figure 21 for two liquid velocities. They characterize the distribution of small gas bubbles in the liquid plug. The distribution of φ_p can be seen to be always nonuniform and shows a maximum for an intermediate radius. The location of the maximum is dependent on the liquid velocity and void fraction. In increasing velocity, the maximum shifts typically to the wall. The distributions of the gas in the liquid plug does not correspond at all to the total local void fraction which is given in figure 14. At the same time, the profile $\varphi_p(r)$ strongly differs from the possible distributions of the gas in a bubble upward flow. In the latter case the gas concentrates much nearer to the wall and the maximum is sharper.

The liquid-velocity profiles in a liquid plug u_p are qualitatively the same as the resultant velocity profiles given in figures 15 and 16. Profiles of u_p are more filled than those of u. Nevertheless, they are located markedly lower than the single-phase turbulent profile in the pipe. In figure 22 the profiles of u_p are plotted on the universal semilog coordinates of "the law of the wall." The value of u_τ was taken as $(\tau_p/\rho_l)^{1/2}$. Here τ_p is the mean value of τ_w at the moments of the passage of liquid plugs, and ρ_l and ν_l are the liquid density and viscosity, respectively. The profiles of u_p are seen to substantially differ from the universal distribution, particularly, in the slope. It is interesting to note that at $yu_\tau/\nu_l < 100$ the profiles corresponding to the same values of $\bar{\gamma}_l$ and different α_m practically coincide. Hence the liquid-velocity distribution for liquid plugs in a vertical flow noticeably differ from that of a fully developed single-phase pipe flow.

3.6 Behavior of instantaneous values of wall shear stress and velocity

The records of the signals from the wall shear stress and velocity probes (figure 10) give us only a rough qualitative idea about the behavior of these parameters in time due to the nonlinearity of the calibration curves. In this paragraph examples will be given for reconstructed records of wall shear stress and velocity. Linearization of signals was performed numerically using the calibration curves given in section 2.

Figure 23 shows records of the wall shear stress, obtained by the above method, as a function of time. Considerable "jumps" of V_τ corresponding to the change of the flow direction have disappeared due to the strongly nonlinear caibration curve $\tau_w(V_\tau)$. The transition from the forward flow to the backward one, occurring in the falling liquid film, is very smooth and is not accompanied by any peculiarities. The reverse transition from the backward flow to the forward one is rather sudden and burst-like. In most cases considerable wall shear stress fluctuations occur in this interval of the record.

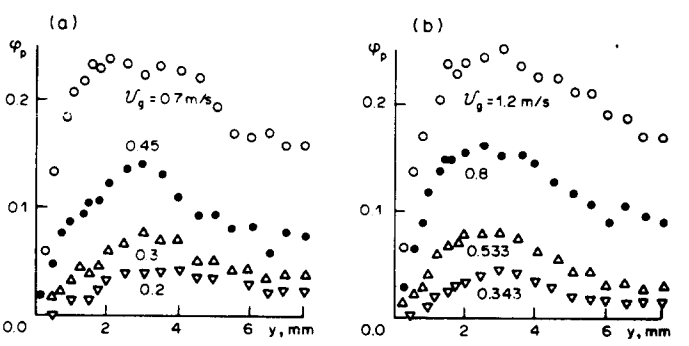

Figure 21. Void fraction in liquid plugs. α, $\bar{\gamma}_l$ = 0.3 m/s; β, $\bar{\gamma}_l$ = 0.8 m/s.

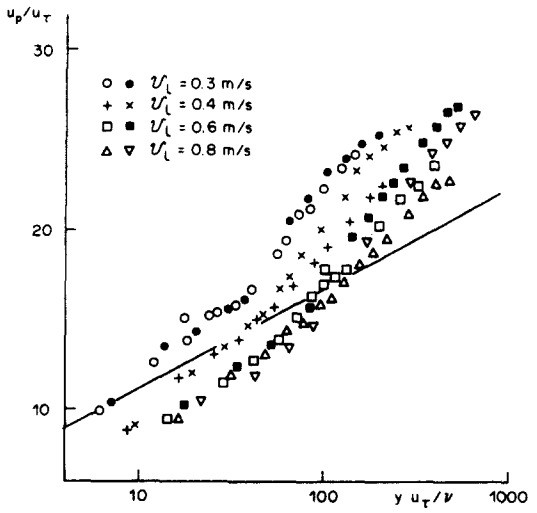

Figure 22. Velocity profiles in liquid plugs in universal semilog coordinates.

When gas slugs are long, the instantaneous values of τ_w in the laminar film (if fluctuations are lacking) reach at the end of a slug some limiting value.

An interesting feature of the records is the behavior of $\tau(t)$ in the range of negative values when the length of a bubble is great. Nearer to the end of the slug, sharp and rather momentary ejections of $\tau(t)$ occur. Such ejections occur only in the region of the film falling downwards and seem to correspond to the moments when the flow becomes unstable and the transition to the turbulent flow begins. Visual observations of the flow in these regimes showed that the film surface at the end of a gas slug is wavy, the quantity of wave perturbations in the film being equal not to one, as predicted by Bretherton (1961), but to several.

Figure 24 shows examples for simultaneous record of the wall shear stress and of the velocity on the pipe axis. Immediately after the passage of a slug there occurs a sharp increase in the liquid velocity and then a smooth decrease up to an approximately constant value at the end the liquid plug. This "average" pattern is superimposed by turbulent

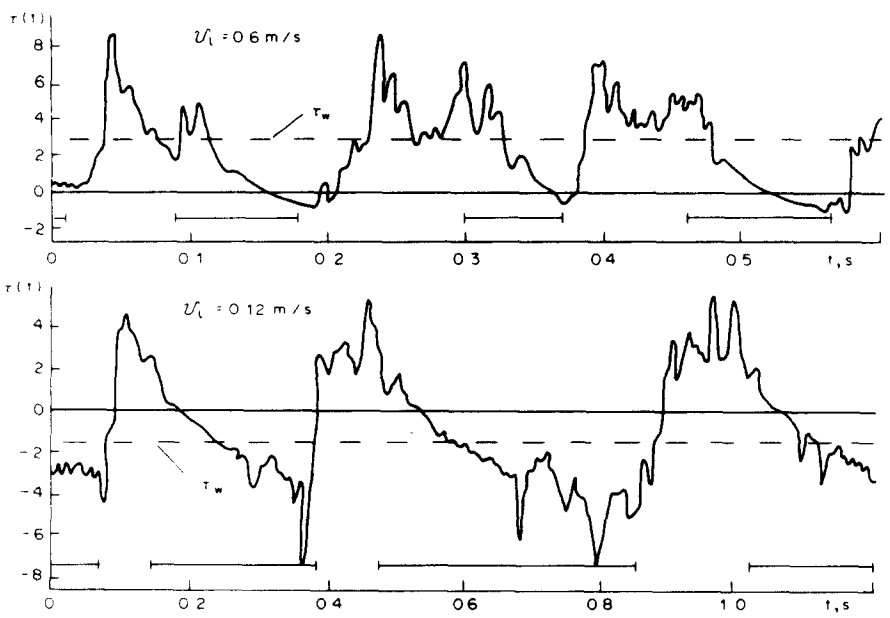

Figure 23. Reconstructed records of wall shear stress. $\tau(t)$, N/m^2; t, s.

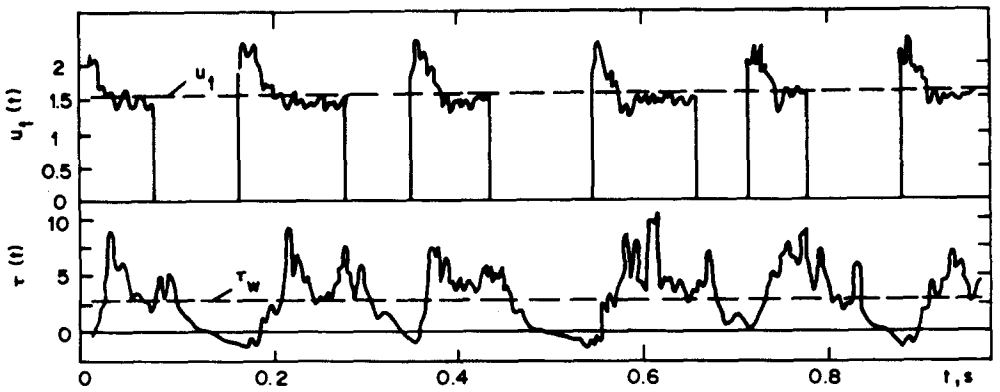

Figure 24. Synchronous records of wall shear stress and axial liquid velocity. $u(t)$, m/s; $\tau(t)$, N/m^2; t, s.

fluctuations. Such a behavior of $u(t)$ is due to the increased value of the longitudinal liquid-velocity component as compared with single-phase flow (the most striking difference takes place in the central part of the pipe). The increase in the velocity on the axis after the passage of a gas slug is rather sudden, whereas the wall friction stress increases with a considerable delay.

The liquid-velocity distribution in liquid plugs is similar. At the distance of $y \geqslant 4$ mm the record of a signal from the velocity probe is qualitatively similar to that of a signal from the probe located on the axis, and after the passage of a slug there is an increase in velocity. While approaching the wall, the instantaneous velocity maximum shifts from the beginning of the liquid plug to its middle. The record of a signal from the velocity probe located near the wall is, naturally, similar to that of the wall shear stress. It is due to the presence, beyond the bottom of the slug, of a toroidal eddy which typically captures gas bubbles. This eddy brings about a deformation of the profiles of void fraction (gas bubbles are drawn away from the wall) and velocity (the velocity near the wall is lower than in a developed single-phase flow).

Thus the flow at the beginning of the liquid plug has the most complicated pattern. Under the action of a decelerated liquid jet flowing from beneath the slug, the wall layer is destroyed, and a new structure is formed. It is evident that these moments must considerably contribute to all the transfer processes in the slug flow.

4. CONCLUSION

A detailed investigation has been carried out into the basic local turbulent characteristics of the slug regime in an upward gas–liquid flow. The local wall shear stress (or surface velocity gradient) has been shown to be characterized by a complicated time behavior, including a possible change of sign at the moments of the passage of a gas slug and at the beginning of the subsequent liquid plug. At low liquid velocities near the wall the liquid, on the average, moves downwards.

Simultaneous records of the liquid velocity and wall shear stress as a function of the time showed that the flow in a liquid plug is divided into two regions: (1) the region immediately after the gas slug, which is characterized by a sharp increase in the velocity on the axis and by a low value of the wall shear stress (the toroidal eddy region beyond the slug) and (2) the liquid plug region, bordering on the beginning of the following slug, where the flow is similar to a common pipe flow. The existence of the first region in the liquid plug determines the high values for the intensity of longitudinal velocity fluctuations as compared with single-phase flow, whereas the intensity of transverse velocity fluctuations does not practically increase.

The measurement results point out that in analyzing the slug-flow fluctuation characteristics, it would be reasonable to distinguish between large-scale perturbations and the intrinsic turbulence of the liquid.

NOMENCLATURE

f_B	backward flow index
R,r	pipe radius, actual radius, mm
t	time, s
T	measurement time, s
T_+,T_-	times of forward and backward flows, s
T_L,T_G	times of liquid plug and gas slug passage in a given cross-section, s
u	liquid velocity, m/s
u_1	axial liquid velocity, m/s
$\mathscr{V}_G,\mathscr{V}_l$	superficial gas and liquid velocities, m/s
$\mathscr{V}_0$	relative gas slug velocity, m/s
$\mathscr{V}_B$	slug velocity, m/s
u',v'	RMS values of longitudinal and transverse components of liquid velocity fluctuations, m/s
V_u,V_τ	voltages, V
y	distance from the wall, mm
α	local void fraction
α_a	local axial void fraction
α_m	mean cross-sectional void fraction
ϵ_u	turbulence index of liquid velocity
$\tau(t)$	instantaneous wall shear stress, N/m^2
τ_+,τ_-	intensities of forward and backward wall shear stresses, N/m^2
τ_L,τ_G	intensities of wall shear stress in liquid plugs and beyond gas slugs, N/m^2
τ_0	single-phase wall shear stress, N/m^2
τ_w	time-averaged wall shear stress in two-phase flow, N/m^2
τ_{wf}	fictitious wall shear stress obtained due to "rectifying" effect, N/m^2
τ'	RMS intensity of wall shear stress fluctuations, N/m^2

Acknowledgement— The authors express their gratitude to S. S. Kutateladze, who stimulated these studies to be performed, for his valuable criticisms and discussions.

REFERENCES

ARMAND, A. A. 1946 Pressure drop in a two-phase flow in horizontal pipes. *Izv. vses. teplotekh. Inst.* **1**, 16–23.

BATCHELOR, G. K. 1970 *An Introduction to Fluid Dynamics*. Cambridge University Press.

BRETHERTON, F. P. 1961 The motion of long bubbles in tubes. *J. Fluid Mech.* **10**, 166–188.

COGNET, G., LEBOUCHE, M. & SOUHAR, M. 1978 Utilisation des techniques electrochimiques pour la mesure de frottement parietal dans les ecoulements diphasiques. *Houille Blanche*, No. 5, 319–322.

DUKLER, A. E. & HABBARD, M. G. 1975 A model for gas–liquid slug flow in horizontal and near horizontal tubes. *Ind. Eng. Chem. Fund.* **14**, 337–347.

ELIN, N. N. & KLAPCHUK, O. V. 1980 On the hypothesis of large-scale motion for gas–liquid flow. *Zh. Prikl. Mekh. Tekh. Fiz.*, No. 4, 114–120.

HANRATTY, T. J. 1967 Study of turbulence close to a wall. *Phys. Fluids Suppl.* **10**, 126–133.

HEWITT, G. F. & HALL-TAYLOR, N. S. 1970 *Annular Two-Phase Flow*. Pergamon, Oxford.

INOUE, A. & AOKI, S. 1976 Void fraction and liquid and gas velocity distribution in bubble flow in a vertical pipe. *Trans. JSME* **42**, 2521–2531.

KARABELAS, A. J. & HANRATTY, T. J. 1968 Determination of the direction of surface velocity gradients in three-dimensional boundary layers. *J. Fluid Mech.* **34**, 159–162.

KASHINSKY, O. N. KOZMENKO, B. K. & NAKORYAKOV, V. E. 1981 Study of fluctuational characteristics of upward gas–liquid flow. *Zh. Prikl. Mekh. Tekh. Fiz.*, No. 6, 67–71.

KUTATELADZE, S. S., BURDUKOV, A. P., NAKORYAKOV, V. E. & KUZMIN, V. A. 1968 Application of electrochemical method of friction measurement in hydrodynamics of two-phase mixtures. In *Heat and Mass Transfer*, A. A. Luikov & B. M. Smolsky (Eds), Vol. 2, pp. 367–375. Nauka i Tekhnika, Minsk, U.S.S.R.

KUTATELADZE, S. S. & STYRIKOVICH, M. A. 1976 *Hydrodynamics of Gas–Liquid Systems.* Energia, Moscow.

LAUFER, J. 1954 The structure of turbulence in fully developed pipe flow. *NACA Rep.* 1174.

MAMAYEV, V. A., ODISHARIA, G. E., KLAPCHUK, O. V., TOCHIGIN, A. A. & SEMYONOV, N. I. 1978 *Motion of Gas–Liquid Mixtures in Pipes.* Nedra, Moscow.

MOISSIS, R. & GRIFFITH, P. 1962 Entrance effects in a two-phase slug flow. *Trans. ASME J. Heat Transfer* C **84**, 29–38.

NAKORYAKOV, V. E., KASHINSKY, O. N., MALKOV, V. A. & KOZMENKO, B. K. 1980 Investigation of characteristics of electrochemical probes for two-phase flow measurements. In *Experimemtal Procedure and Apparatuses for Turbulence Investigations*, S. S. Kutateladze (Ed.), pp. 27–35. Novosibirsk, U.S.S.R.

NAKORYAKOV, V. E., KASHINSKY, O. N., BURDUKOV, A. P. & ODNORAL, V. P. 1981 Local characteristics of upward gas–liquid flow. *Int. J. Multiphase Flow* **7**, 63–81.

SATO, Y. & SEKOGUCHI, K. 1975 Liquid velocity distribution in two-phase bubble flow. *Int. J. Multiphase Flow* **2**, 79–95.

SERIZAWA, A., KATAOKA, I. & MICHIYOSHI, I. 1975 Turbulent structure of air–water bubbly flow. *Int. J. Multiphase Flow* **2**, 235–246.

WALLIS, G. B. 1969 *One-Dimensional Two-Phase Flow*. McGraw-Hill, New York.